Jakson P. BONALDO[1], Helmo K. M. PAREDES[2], José A. POMILIO[3]

UTFPR – Federal University of Technology - Parana (1), UNESP – Sao Paulo State University (2), UNICAMP – University of Campinas (3)

doi:10.15199/48.2015.03.34

Multifunctional Current Reference Generation Strategy for Grid-tied Power Electronic Converter

Abstract. *In this work the functionalities of Power Electronic Converters (PEC) used as grid interface device for distributed generation sources are extended to deal with Power Quality (PQ) issues. It is proposed an alternative strategy to obtain current references based on the Conservative Power Theory (CPT). The proposed strategy contributes to the full exploitation of the PEC power capacity, allowing the PEC to act as a multifunctional device performing simultaneously selective compensation of PQ issues and power injection into the utility grid.*

Streszczenie. *Elektroniczny konwerter mocy PEC używany jako interfejs rozproszonych źródeł energii został poszerzony o możliwości poprawy jakości energii. Prądowe źródło odniesienia bazuje na Teorii Zachowania Mocy CPT.* ***Wielofunkcyjne prądowe źródło odniesienia do sieciowego konwertera mocy.***

Keywords: multifunctional power converter, power quality, renewable power sources, selective compensation.
Słowa kluczowe: konwerter mocy, rozproszone systemy zasilania, jakośc energii.

Introduction

Nowadays, power electronic converters (PEC) used as power electronic interface (PEI) between the grid utility and the renewable energy sources (RES) are experiencing an increasing evolution in terms of their functionalities. In addition to the current injection into the grid, these converters are also being used to improve the power quality at point of common coupling (PCC) [1-3]. Usually, it is desired the injection of full power available from the RES into the grid. If the RES´s power is less than the converter power rating the remaining available power may be used to compensate for power quality disturbances, like harmonics pollution and reactive power [4-7].

Fig. 1 shows a structure commonly used to inject small amounts of active power into the grid, which is largely used with solar cells [8, 9]. This system could also be adapted to perform power quality (PQ) tasks by acting as an active power filter (APF). This is possible by changing only the control laws and feeding back the load current which could be decomposed following some specific criteria and generate the current references for PQ compensation, power injection or both simultaneously.

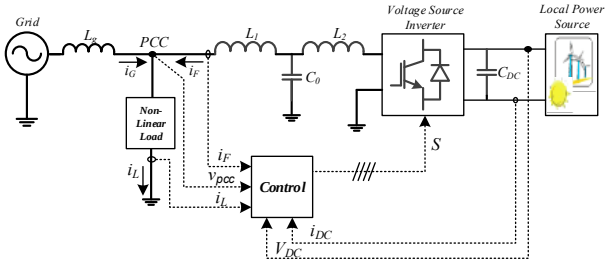

Fig. 1 – Overview of the multifunctional power electronic converter.

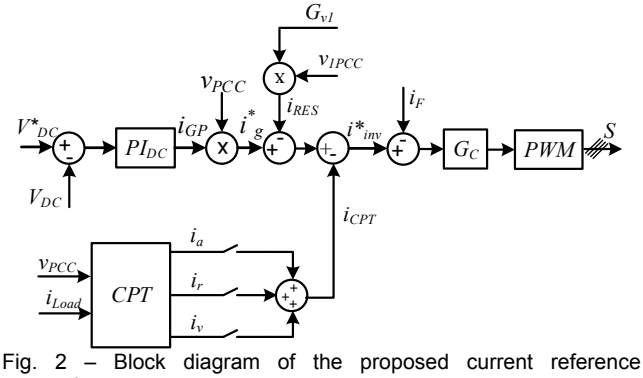

Fig. 2 – Block diagram of the proposed current reference generation.

However, when the PEC acts simultaneously as power injection and PQ disturbances compensation device, the available power capability of the PEC might not be enough to deal with all the concerns occurring at PCC. Therefore, some selective compensation strategies could be used, where the compensation level would be directly related to the available PEC capability i.e. the remaining power capability which is not being supplied to the grid is used for selective compensation. The current reference for compensation can be generated by using an approach consisting of complex digital filters [10], harmonic damping methods [7] or well known power theories [11,12].

In this paper the Conservative Power Theory (CPT) [13,14] is used as an alternative to generating different current references for selective disturbances compensation and active power injection from local renewable source. Fig. 2 shows the proposed strategy for current generation. The CPT current decompositions result in several current-related terms associated with specific load characteristics. These current terms are orthogonal (decoupled) and could be used by the control system to generate the current reference for selective compensation.

Simulations and experimental analysis are both performed considering a non-linear load under non-sinusoidal weak grid (characteristic of a microgrid) with inductance and resistance of considerable values [15]. In Table I the main parameters of the system are presented. For the sake of simplicity, the series resistances of inductors and capacitors are not shown in the Fig. 1, but its values are presented in table I. This structure is adopted because it is very common in low voltage distribution networks, which are the propitious places for connection of small power distributed generation units.

Table 1. System Parameters

Parameter	Value
Inductance of the LCL filter, L_1, L_2	0.5 mH
Resistance of the inductors of the LCL filter, R_1, R_2	100 mΩ
Capacitance of LCL filter, C_o	3 uF
Equivalent series resistance of C_o, R_o	10 mΩ
Grid inductance, L_g	2 mH
Grid resistance, R_g	200 mΩ
Coupling inductance of the non-linear load, L_C	1 mH
Inductance of the linear load, L_L	70 mH
Resistance of non-linear load R_L	70 Ω
Capacitance of the non-linear load, C_L	470 uF
DC bus voltage, V_{DC}	300 V
DC bus capacitance, C_{DC}	1 mF

Overview of the CPT Current Decomposition

The Conservative Power Theory (CPT), proposed in [13, 14] is defined on the time domain. It is suitable to be applied on non sinusoidal and unbalanced periodic waveforms of period T and angular frequency $\omega=2\pi/T$ and can also be applied on poly-phase systems, with or without return conductor. The CPT proposes an orthogonal (decoupled) current's decomposition based on two conservative quantities, which are the active power (P) and the reactive energy (W). For this, the authors introduced, the unbiased voltage integral, $\hat{v}(t)$ that corresponds to integral of $v(t)$ without the mean value, as defined in (1).

$$\hat{v}(t) = v_{int} - v_0 \tag{1}$$

$$v_{int}(t) = \int_o^t v(t)dt \tag{2}$$

$$v_o = \frac{1}{T}\int_0^t v_{\text{int}}(t)dt \tag{3}$$

Where $v_{int}(t)$ is the integral of the voltage and v_o is the mean value of $v_{int}(t)$.

Considering single phase system, the active power, P is defined in (4) and related to the average power transfer, with $v(t)$ and $i(t)$ representing instantaneous voltage and current.

$$P = \frac{1}{T}\int_0^T v(t)i(t)dt \tag{4}$$

Reactive energy, W, is defined in a similar way to the active power, but instead of voltage, it uses the unbiased voltage integral as shown in (5):

$$W = \frac{1}{T}\int_0^T \hat{v}(t)i(t)dt \tag{5}$$

The reactive energy term represent the power fluctuations and current flow caused by energy storage elements. Notice that, equation (5) is valid for any voltage and current waveforms (either sinusoidal or not). Under sinusoidal conditions, this phenomenon is accounted by traditional reactive power Q, as defined in (6).

$$Q = VI\sin(\theta) = \omega W \tag{6}$$

The active power and reactive energy form the bases to the orthogonal current decomposition where each component maintains a specific physical meaning. Thus, the current of a generic network can be decomposed into: active current (i_a), reactive current (i_r) and void current (i_v).

Active current is defined as the minimum current (i.e. with minimum RMS value) required to convey active power P absorbed from network and is given by (7). Where V is the RMS value (norm) of voltage and G_e is called equivalent conductance.

$$i_a = \frac{P}{V^2}v = G_e \cdot v \tag{7}$$

Reactive current is defined as the minimum current (i.e. with minimum RMS value) required to convey reactive energy W absorbed form network and is given by (8). Where $\hat{V}$ is the RMS value of unbiased voltage integral and B_e is called equivalent reactivity. Under sinusoidal conditions equivalent reactivity is identical to susceptance.

$$i_r = \frac{W}{\hat{V}^2}\hat{v} = B_e \cdot \hat{v} \tag{8}$$

The void current is given by (9), it is also called residual current, since it is neither conveying active power nor reactive energy. Thus, this current component reflects the presence of harmonics, which are due to nonlinear loads or voltage distortion [16].

$$i_v = i - i_a - i_r \tag{9}$$

In conclusion, the current can be decomposed as (10).

$$i = i_a + i_r + i_v \tag{10}$$

By definition, these current components are orthogonal, thus their RMS values lead to (11).

$$I^2 = I_a^2 + I_r^2 + I_v^2 \tag{11}$$

Finally, the apparent power may be calculated as (12).

$$A^2 = V^2 I_a^2 + V^2 I_r^2 + V^2 I_v^2 = P^2 + Q^2 + D^2 \tag{12}$$

The power terms in (12) are depicted as: $P=VI_a$ is active power and related to the average power transfer. $Q=VI_r$ is reactive power and related to the reactive energy and $D=VI_v$ is void power and related to load nonlinearities and voltage distortion. Unlike active power and reactive energy, apparent, reactive and void powers are not conservative quantities [13,14].

Generation of Current References for Compensation and Power Injection

The local renewable power source could be a photovoltaic array, a fuel cell or a wind generator. However, in this paper, the local source is modelled as a DC current source, I_{DC}. The current reference for power injection, i_{RES}, which is related to the active power as shown in (7), is used to inject the power delivered by I_{DC} into the grid through the PEC. As shown in (13), i_{RES} follows the voltage waveform at point of connection of the PEC. In general, the waveform of the active current reference (i_{RES}) can be defined either from the measured PCC voltage ($v=v_{PCC}$) or from its fundamental component ($v=v_{1PCC}$), configuring resistive or sinusoidal current injection, respectively.

$$i_{RES} = \frac{P_{DC}}{V^2}v = G_v \cdot v \tag{13}$$

The overall current reference (i^*_{inv}) which should be synthesized by the PEC is given by (14). Fig. 2 shows a schematic summarizing the reference generation strategy.

$$i^*_{inv} = i^*_g + i_{RES} - i_{CPT} \tag{14}$$

The current reference i^*_g represents the current needed to keep the DC voltage regulated and grant the power balance between DC and AC sides of PEC. The reference i^*_g is generated by the product of the peak current (generated by PI_{DC}).

Note that in (14), the CPT current decomposition can provide the current reference (i_{CPT}) to compensate, selectively or not, the load current disturbances. The reference for disturbance compensation is generated according (8) and (9), as shown in (15). If it is required to compensate only the harmonics due to the load current, the reference for compensation is given by $i_{CPT}=i_v$.

$$i_{CPT} = i_r + i_v \tag{15}$$

(16) $$G_F(s)=\frac{I_F(s)}{V_{INV}(s)}=\frac{sC_oR_o+1}{s^3C_oL_1L_2+s^2C_o\begin{pmatrix}L_1R'_2+L'_2R_1+\\+L_1R_o+L'_2R_o\end{pmatrix}+sC_o\begin{pmatrix}L_1+L'_2+R'_2R_1+\\+R_1R_o+R'_2R_o\end{pmatrix}+R_1+R'_2}$$

PEC Modelling and Control

In this section the current controlled voltage source inverter is designed and modelled. PEC control system consists of two feedback control loops. The first is a fast loop which controls the output current [17] and the other is a slower loop which keeps constant the DC bus voltage [18, 19]. A secondary loop controls the current injection of RES in the DC bus.

Output Current control

Fig. 3 shows the block diagram of the inverter's current control loop. The transfer function relating the current, flowing through the output inductor of the LCL filter and the inverter voltage is shown in (16). The open loop transfer function $G_{OL}(s)$ is obtained taking into account the time delay due to the PWM modulator, $G_{PWM}(s)$. Since this controller is intended to be implemented on a DSP platform, it should be also considered the delay due to the control algorithm processing time given by $G_d(s)$, and the anti-aliasing filter given by $G_a(s)$, which is placed at the input of the analog-to-digital converter (ADC). The inverter gain is K_{inv}, while K_{IS} is current sensor gain. The cutoff frequency of anti-aliasing filter is ω_{c_anti}. The sampling time is given by T_s.

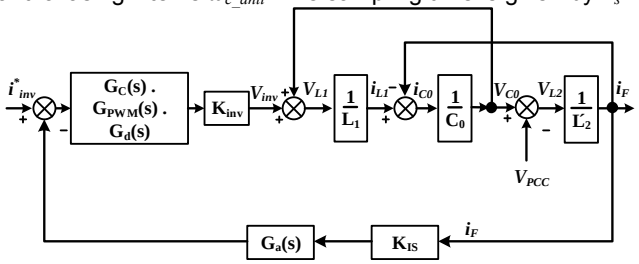

Fig. 3 - Block diagram of output current control.

(17) $$G_{OL}(s)=K_{IS}K_{INV}G_{PWM}(s)G_F(s)G_a(s)G_d(s)G_C(s)$$

(18) $$G_d(s)=\frac{1-s\frac{2}{4}T_s}{1+s\frac{2}{4}T_s}$$

(19) $$G_{PWM}(s)=\frac{1-s\frac{1}{4}T_s}{1+s\frac{1}{4}T_s}$$

(20) $$G_a(s)=\frac{\omega_{c\_anti}}{s+\omega_{c\_anti}}$$

The current controller $G_c(s)$ is based on the proportional resonant plus harmonic controller (PR+HC) [20, 21]. The proportional and integral gains of resonant controller are K_C and K_{IPR}, respectively. The bandwidth of each resonant frequency is denoted by ω_{cPR}, h is the harmonic order and ω_o is fundamental frequency of the grid utility. This controller is designed considering that, above the resonant frequency, the LCL filter and consequently $G_{OL}(s)$, behaves like an inductance. Thus, the LCL filter can be simplified to a total inductance given by (22). Thus, K_C is calculated by (23). The target cutoff frequency of closed loop is ω_{CL}.

(21) $$G_C(s)=K_C+\sum_{h=1}^{15}\frac{2sK_{IPR}\omega_{CPR}}{s^2+2s\omega_{CPR}+(h\omega_o)^2}$$

(22) $$L_T=L_1+L_2$$

(23) $$K_C=\frac{\omega_{CL}L_T}{K_{INV}K_{IS}}$$

Table 2 shows the values used on the current controller and Fig. 4 shows the frequency response of the open loop transfer function, $G_{OL}(s)$, before and after compensation with $G_c(s)$. The phase margin is about 45° and the gain margin is about 6 dB. The bandwidth of the current loop is 1 kHz.

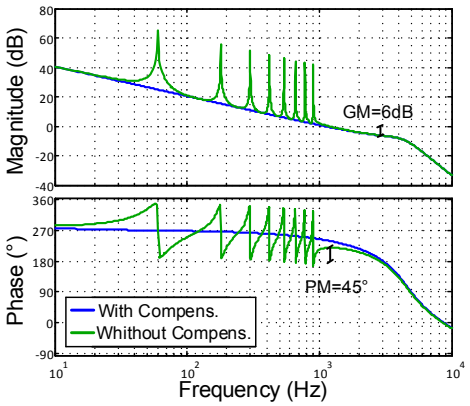

Fig. 4 - Current open loop transfer function before and after compensation.

Table 2. Parameters of Current Controller

Parameter	Value
Inverter gain, K_{INV}	300
Current sensor gain, K_{IS}	0.0667
Sampling time, T_s	38 us
Cutoff frequency of anti-aliasing filter, ω_{c_anti}	62.8 krad/s
Grid frequency, ω_o	377 rad/s
Bandwidth of the resonant controller, ω_{cPR}	5 rad/s
Proportional gain of resonant controller, K_C	0,95
Integral gain of resonant controller, K_{IPR}	100
Cutoff frequency of current closed loop, ω_{CL}	6.28 krad/s

DC bus voltage control

The DC link keeps the power balance between the power which is delivered to the system in the output of the PEC and the power in the DC link, even when the converter is acting only as an APF. Fig. 5 shows the block diagram of the DC voltage control loop.

The transfer function $G_{DC}(s)$ is obtained by using a small signal analysis, it establishes a relationship between the DC link voltage, V_{DC}, and the current peak at the inverter output i.e. current control variable I_{Gp}. The low-pass filter, $H_{LP}(s)$, in the feedback path is designed to attenuate the 120 Hz ripple present in the V_{DC} voltage. In this work the cutoff frequency of the low pass filter is $\omega_{cLP}=30Hz$. Fig. 6 shows the transfer function of the DC link voltage with and without PI compensator.

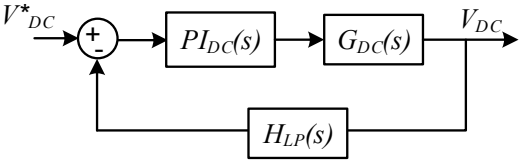

Fig. 5 - Block diagram of DC voltage control.

(24) $$G_{DC}(s) = \frac{\tilde{v}_{DC}(s)}{\tilde{i}_{RP}(s)} = \frac{V_{DC}}{2\sqrt{2}C_{DC}V_{DC}^{*}}$$

(25) $$H_{LP}(s) = \frac{\omega_{CLP}}{s + \omega_{CLP}}$$

(26) $$PI_{DC}(s) = K_P + \frac{K_I}{s}$$

(27) $$H_{DC_{CL}}(s) = \frac{G_{DC}(s)PI_{DC}(s)}{1 + G_{DC}(s)PI_{DC}(s)H_{LP}(s)}$$

The bandwidth was set to 6Hz, and the requirement for the phase margin was set to 70° in order to obtain a compensated system with small overshoot. The parameters of $PI_{DC}(s)$ are $K_P=2.2$ and $K_I=49$. The peak of grid voltage is $180V$ and the reference voltage for the DC link is $V^*_{DC}=300V$.

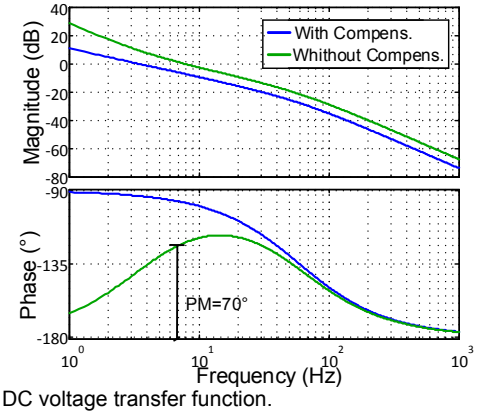

Fig. 6 – DC voltage transfer function.

Experimental Results

In order to validate the approach proposed in this work, a prototype of the system shown in Fig. 1 has been implemented and tested. Fig. 7.a shows the DC bus voltage, grid current and current at output of PEC. At (1) the current source I_{DC} is connected to the DC bus injecting 2A. At (2) a load step is applied, since the non-linear load is disconnected from PCC. Finally, at (3) the non-linear load is re-connected to the PCC. Fig. 7.b shows details of the waveforms.

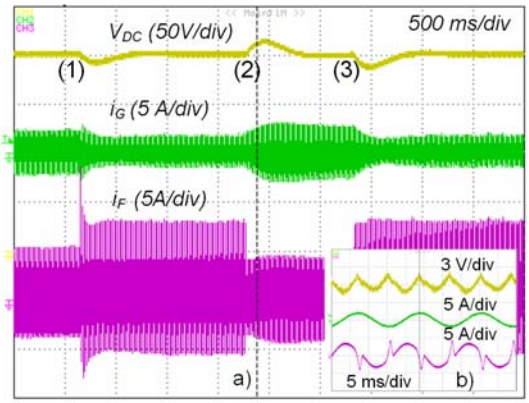

Fig. 7 – Dynamic behavior: a) DC link voltage, grid current and PEC current; b) Detail of steady state ripple .

In order to show the system selective compensation capability, it is analyzed the three feasible compensation modes. The operation only as an APF, operation only as PEI and operation as APF and PEI simultaneously. The I_{DC} source is built based on a current controlled boost topology, the input is composed of 150V voltage source. The proposed system has been tested on the lab electrical grid, which is 60 Hz / 127 V grid polluted with 1.8% of 5th harmonic and 0.5% of 7th harmonic. The THD of the grid is about 1.8%.

PEC operating only as APF

In this mode of operation the PEC works only as an APF i.e. there is no injection of active power into the grid. With the PEC turned off, Fig. 8 shows the PCC voltage (V_{PCC}), the grid current (i_G) and the current at the output of the PEC (i_F). Notice that, both voltage and current are distorted. Fig. 9 shows the waveforms when the system is compensating only reactive power, since the PEC is providing only reactive component from load current. Observe that, the current at PCC (i_G) remains distorted, however in phase with the PCC voltage. Fig. 10 shows the compensation only of the void current, which is related to harmonics of current. In this case, i_G has the same waveform of V_{PCC}, but it is not in-phase with PCC voltage. Moreover, one can realize that the disturbances associated with the voltage were also compensated, since they were in part imposed by the load. Finally, Fig. 11 brings the result of the full compensation, where the void and reactive current are being compensated simultaneously. Notice that in Fig. 11 the current at PCC (i_G) has the same waveform of V_{PCC}.

Table 3 shows the main performance parameters and Fig. 12 shows the harmonics spectrum of the grid current (i_G) considering the different compensation strategies. It is worth to observe that the THD of the current when the PEC is performing only the reactive compensation is greater than when the PEC is turned off. This effect is caused by the decrease in the fundamental component of grid current and also because the harmonic components remain unchanged, since there is no change in the load. Another interesting behaviour is that, when the PEC is performing the void current compensation, we obtained the best performance in terms of THD, moreover the power processed by the PEC is lower than other strategies.

A load step is shown in Fig. 13. The reactive load is switched off. Besides the slow response of the DC voltage control, the grid current achieve the steady state in few cycles.

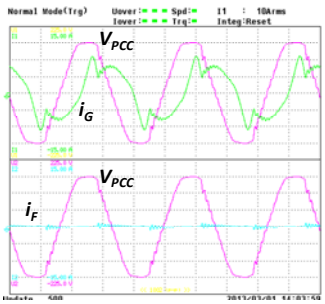

Fig. 8 - PCC voltage (V_{PCC}), grid current (i_G) and PEC current (i_F) when PEC is off.

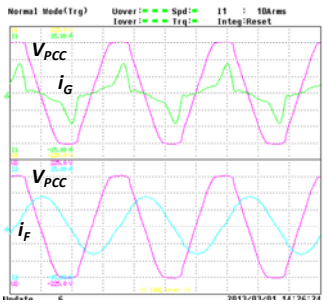

Fig. 9 - PEC operating as APF, for reactive current (i_r) compensation.

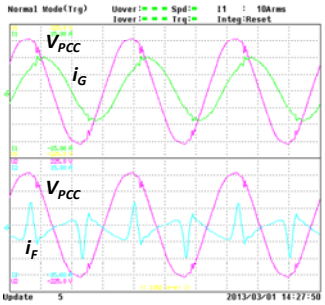

Fig. 10 - PEC operating as APF for void current compensation.

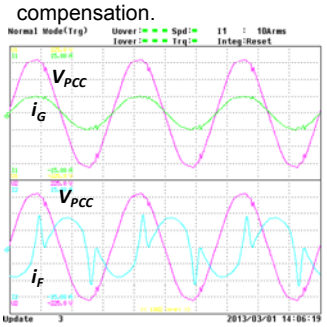

Fig. 11 - PEC operating as APF for full compensation.

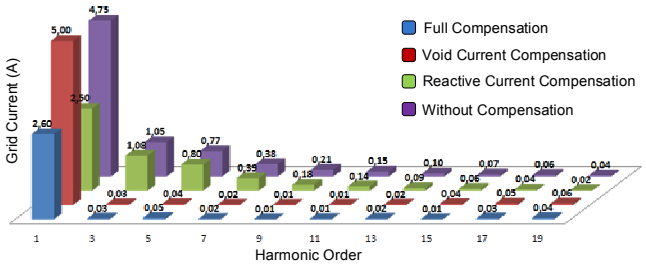

Fig. 12 – Harmonic spectrum of the grid current when the PEC is operating as APF for different compensation strategies.

Table 3. PEC Operation only as APF

Parameter	Compensation Type			
	none	reactive	void	full
P_g *[W]*	242	318	304	335
Q_g *[VAR]*	540	20	587	34
S_g *[VA]*	590	319	660	336
P_{PEC} *[W]*	1	60	-50	-73
Q_{PEC} *[VAR]*	17	560	249	550
S_{PEC} *[VA]*	17	564	254	555
V_{PCC} *[V]*	125.978	128.813	125.387	128.750
I_G *[A]*	4.9705	2.8749	5.0533	2.6186
V_{1PCC} *[V]*	125.7	128.6	125.3	128.7
I_{G1} *[A]*	4.75	2.5	5.0	2.6
THD V_{PCC} *[%]*	5.6	5.0	3.0	2.7
THD I_G *[%]*	30	57	3.5	4.9

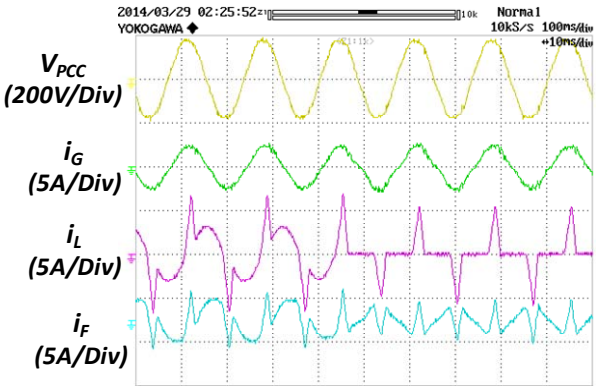

Fig. 13 – Load transient: reactive load disconnected.

PEC operating as PEI and APF simultaneously

When the current source I_{DC} is connected to the DC bus, the PEC begins to operate as a multifunctional converter, i.e. injecting active power from local source into the grid and compensating the unwanted current components of the nonlinear load. For this test, the current source is injecting 2 A into the DC bus, giving a total power of 600 W.

Fig. 14 shows the voltage and current waveforms when the PEC is injecting power into the grid without using any compensation strategy. As expected, the PEC current, i_F, is sinusoidal because the fundamental component of PCC is being used to generate the current reference for power injection, as shown in Fig. 2. It should be noted that the PCC voltage is distorted not only due to the load current but also due to the fact that the grid voltage, V_G, is distorted (about 1,8%).

From Figs. 15 to 17, we can observe that, the active power injection (PEI functionality), does not affect the performance of the PEC at the different compensation strategies. Thus, it is possible, besides injecting active current (active power) into the grid, obtain a selective compensation of the unwanted currents. Additional information about the performance of the PEC, when acting as PEI and APF simultaneously can be found in the table 4 and Fig 18.

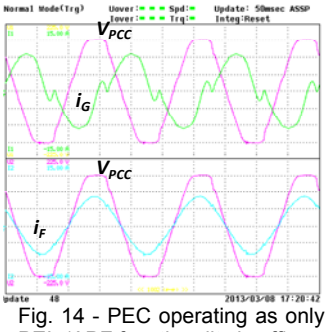

Fig. 14 - PEC operating as only PEI. (APF functionality is off).

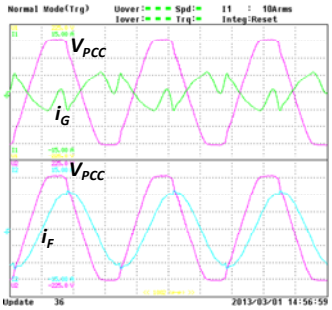

Fig. 15 - PEC operating as PEI and APF (reactive compensation).

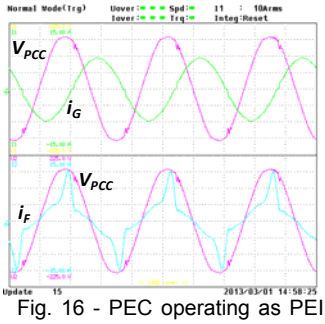

Fig. 16 - PEC operating as PEI and APF (void compensation).

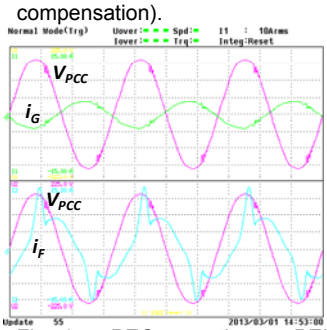

Fig. 17 - PEC operating as PEI and APF (full compensation).

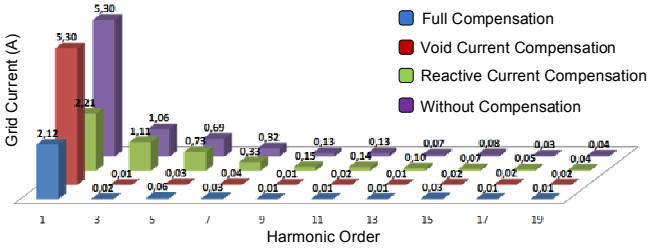

Fig. 18 – Harmonic spectrum of the grid current when the PEC is operating as PEI and APF using different compensation strategies.

Table 4. PEC Operation as APF and PEI simultaneously

Parameter	Compensation Type			
	none	reactive	void	full
P_g *[W]*	-318	-294	-309	-280
Q_g *[VAR]*	613	28	613	25
S_g *[VA]*	680	295	686	282
P_{PEC} *[W]*	573	560	573	557
Q_{PEC} *[VAR]*	-19	592	-35	591
S_{PEC} *[VA]*	574	815	574	812
V_{PCC} *[V]*	128.93	132.48	128.76	132.27
I_G *[A]*	5.472	2.608	5.335	2.134
V_{1PCC} *[V]*	128.8	132.3	128.7	132.25
I_{G1} *[A]*	5.3	2.21	5.3	2.12
THD V_{PCC} *[%]*	4.6 %	4.9	2.8	2
THD I_G *[%]*	24 %	63	2.0	4.6

PEC Operating only as PEI

If the load is disconnected from the PCC, the system behaves like a standard PEI performing only the injection of the power into the grid, since there are no disturbances to be compensated for as shown in Fig. 19. The THD of the grid current is about 1.4% and the THD of the PCC voltage is about 1.7% which is only due to the polluted grid voltage. Table 5 summarizes the performance data collect in this operation mode.

The performance of the multifunctional converter is similar to the performance achieved using standard PEI. In [22-24] the values of the grid current THD are about 2%, 1.4% and 4%, respectively. The result achieved in the present work is also compatible with other works related to multifunctional use of power converters. In [25], the THD of grid current is 2%, when the converter is operated as a

standard PEI, while in this work the THD of grid current is 1.4%.

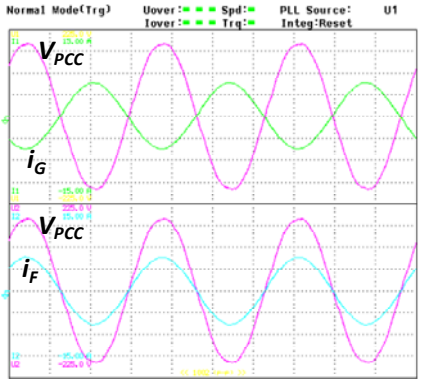

Fig. 19 – PCC voltage (V_{PCC}), grid current (i_G) and PEC current (i_F) when PEC is operating only as PEI injecting power into the grid (there is no load connected to the PCC).

Table 5. PEC Operation only as PEI (No Load)

Parameter	Value	Parameter	Value
P_g *[W]*	-558	V_{PCC} *[V]*	132.93
Q_g *[VAR]*	34	I_G *[A]*	4.2
S_g *[VA]*	559	V_{1PCC} *[V]*	132.82
P_{PEC} *[W]*	573	I_{G1} *[A]*	4.2
Q_{PEC} *[VAR]*	-18	THD V_{PCC} *[%]*	1.7
S_{PEC} *[VA]*	574	THD I_G *[%]*	1.4

Conclusions

In order to comply with the rated capacity of the PEC, there are situations in which it is not possible to perform the full compensation of disturbances along with power injection. Therefore, either the disturbances compensation or the power injection into the grid should be limited.

Thus, due to the CPT, it is possible to decompose the power related to the disturbances and, based in some criteria which could be the rated power of the PEC or its current capability, choose the power components to be compensated. The full compensation could be achieved if the PEC has enough capacity available, providing that the maximum current and voltage capacity are not violated. In the case that the PEC is overrated the reactive compensation could be performed by passive elements like capacitors and inductors which are cheaper than the PEC. Then, the PEC would perform the compensation of the void component as well as the remaining reactive component. As observed in the experimental results, a relative small amount of power capacity is needed to compensate the void component, not compromising the capacity need to perform the power injection into the grid.

The results obtained for THD of voltage and current in the PCC considering the multifunctional converter are compatible with those results reported in the cases where a PEC conventionally operated was used. Therefore, this work has shown that with changes only in the current reference generation it is possible to perform selective disturbances compensation simultaneously to the power injection into the grid.

This work was supported by the São Paulo Research Foundation (FAPESP) under grant 2011/15884-6 and 2013/08545-6 and by CAPES and CNPq. The authors also would like to express their thank to Semikron.

REFERENCES

[1] Carnieletto, R.; Suryanarayanan, S.; Simoes, M.G.; Farret, F.A., "A Multifunctional Single-Phase Voltage Source Inverter in Perspective of the Smart Grid Initiative," Industry Applications Society Annual Meeting, 2009. IAS 2009. IEEE, vol., no., pp.1-7, Oct. 2009.

[2] Singh, M.; Khadkikar, V.; Chandra, A.; Varma, R.K., "Grid Interconnection of Renewable Energy Sources at the Distribution Level With Power-Quality Improvement Features," Power Delivery, IEEE Transactions on, vol.26, no.1, pp.307-315, Jan. 2011.

[3] Machado, R.Q.; Buso, S.; Pomilio, J.A.; Marafao, F.P., "Three-phase to single-phase direct connection rural cogeneration systems," Applied Power Electronics Conference and Exposition, 2004. APEC '04. Nineteenth Annual IEEE, vol.3, no., pp. 1547- 1553 Vol.3, 2004.

[4] Piasecki S.; Jasiński, M.; Rafał, K.; Korzeniewski, M., Milicua, A., Higher harmonics compensation in grid-connected PWM converters for renewable energy interface and active filtering, Przeglad Elektrotechniczny, 87 (2011), nr 6, 85-90.

[5] Si-Hun Jo; SeoEun Son; Jung-Wook Park, "On Improving Distortion Power Quality Index in Distributed Power Grids," Smart Grid, IEEE Transactions on, vol.4, no.1, pp.586-595, March 2013.

[6] Von Appen, J.; Stetz, T.; Braun, M.; Schmiegel, A., "Local Voltage Control Strategies for PV Storage Systems in Distribution Grids," Smart Grid, IEEE Transactions on, vol.5, no.2, pp.1002-1009, March 2014.

[7] Munir, S.; Yun Wei Li, "Residential Distribution System Harmonic Compensation Using PV Interfacing Inverter," Smart Grid, IEEE Transactions on, vol.4, no.2, pp.816-827, June 2013.

[8] Bin Gu; Dominic, J.; Jih-Sheng Lai; Chien-Liang Chen; LaBella, T.; Baifeng Chen, "High Reliability and Efficiency Single-Phase Transformerless Inverter for Grid-Connected Photovoltaic Systems," Power Electronics, IEEE Transactions on, vol.28, no.5, pp.2235-2245, May 2013.

[9] Alajmi, B.N.; Ahmed, K.H.; Adam, G.P.; Williams, B.W., "Single-Phase Single-Stage Transformer less Grid-Connected PV System," Power Electronics, IEEE Transactions on, vol.28, no.6, pp.2664-2676, June 2013.

[10] Illindala, M.; Venkataramanan, G., "Frequency/Sequence Selective Filters for Power Quality Improvement in a Microgrid," Smart Grid, IEEE Transactions on, vol.3, no.4, pp.2039-2047, Dec. 2012.

[11] Watanabe, E. H., Alfonso, J. L., Pinto, J. G., Monteiro, L. F. C., Aredes, M., Akagi, H. "Instantaneous p-q power theory for control of compensators in micro-grids," Przeglad Elektrotechniczny, vol. 86, no. 6, pp. 1–10, 2010.

[12] Bitoleanu A. and Popescu M., How The p-q theory and Compensating Current Calculation for Shunt Active Power Filters: Theoretical Aspects and Practical Implementation, Przeglad Elektrotechniczny, v. 89, no. 6, pp. 11-16, 2013.

[13] Tenti, P.; Paredes, H.K.M.; Mattavelli, P., "Conservative Power Theory, a Framework to Approach Control and Accountability Issues in Smart Microgrids," Power Electronics, IEEE Transactions on, vol.26, no.3, pp.664-673, March 2011.

[14] Paredes, H. K. M.; da Silva, L. C. P.; Brandão, D. I.; Marafão, F. P., "Possible Shunt Compensation Strategies Based on Conservative Power Theory", Przeglad Elektrotechniczny, v. 87, p. 34-39, 2011.

[15] Shen, G.; Xu, D.; Cao, L.; Zhu, X., "An Improved Control Strategy for Grid-Connected Voltage Source Inverters With an LCL Filter," Power Electronics, IEEE Transactions on, vol.23, no.4, pp.1899-1906, July 2008.

[16] Marafão, F. P, Souza, W.; Liberado, E.; , Silva, L.; Paredes, H, Load Analyser using Conservative Power Theory, Przeglad Elektrotechniczny, 89 (2013), nr 12, 1-6.

[17] P. Mattavelli and S. Buso. "Digital Control in Power Electronics". 1st ed. Morgan & Claypool Publishers.

[18] Khajehoddin, S.A.; Karimi-Ghartemani, M.; Jain, P.K.; Bakhshai, A., "DC-Bus Design and Control for a Single-Phase Grid-Connected Renewable Converter With a Small Energy Storage Component," Power Electronics, IEEE Transactions on, vol.28, no.7, pp.3245-3254, July 2013.

[19] Curtri, R.; Matakas, L., "Reference currents determination techniques for load unbalance compensation", 7th Brazilian Conference on Power Electronics, 2003.

[20] Yepes, A.G.; Freijedo, F.D.; Lopez, O.; Doval-Gandoy, J., "Analysis and Design of Resonant Current Controllers for Voltage-Source Converters by Means of Nyquist Diagrams and Sensitivity Function," Industrial Electronics, IEEE Transactions on, vol.58, no.11, pp.5231-5250, Nov. 2011.

[21] Hasanzadeh, A.; Onar, O.C.; Mokhtari, H.; Khaligh, A., "A Proportional-Resonant Controller-Based Wireless Control Strategy With a Reduced Number of Sensors for Parallel-Operated UPSs," Power Delivery, IEEE Transactions on, vol.25, no.1, pp.468-478, Jan. 2010.
[22] Araujo, S.V.; Zacharias, P.; Mallwitz, R., "Highly Efficient Single-Phase Transformerless Inverters for Grid-Connected Photovoltaic Systems," Industrial Electronics, IEEE Transactions on, vol.57, no.9, pp.3118-3128, Sept. 2010.
[23] Riming Shao; Kaye, M.; Liuchen Chang, "Advanced building blocks of power converters for renewable energy based distributed generators," Power Electronics and ECCE Asia (ICPE & ECCE), 2011 IEEE 8th International Conference on, vol., no., pp.2168-2174, May 30 2011-June 3 2011.
[24] Buticchi, G.; Lorenzani, E.; Franceschini, G., "A Five-Level Single-Phase Grid-Connected Converter for Renewable Distributed Systems," Industrial Electronics, IEEE Transactions on, vol.60, no.3, pp.906-918, March 2013.
[25] Bojoi, R.; Limongi, L.R.; Roiu, D.; Tenconi, A., "Enhanced Power Quality Control Strategy for Single-Phase Inverters in Distributed Generation Systems," Power Electronics, IEEE Transactions on, vol.26, no.3, pp.798-806, March 2011.

***Authors**: Jakson Paulo Bonaldo, Federal University of Technology - Paraná, Group of Electronic Engineering, Via Rosalina Maria dos Santos, 1233, Zip: 87301-899, Campo Mourão, PR, Brazil, E-mail: jbonaldo@gmail.com;*
prof. dr Helmo Kelis Morales Paredes, Univ Estadual Paulista (UNESP), Campus of Sorocaba, Group of Automation and Integrated Systems, (GASI), Av. Três de Março 511, Zip: 18087-180, Sorocaba – SP – Brazil, E-mail: hmorales@sorocaba.unesp.br;
prof. dr. José Antenor Pomilio, University of Campinas, School of Electrical and Computer Engineering, Campinas, Brazil, E-mail: antenor@dsce.fee.unicamp.br.